



Spectroscopic and dielectric studies of *meso*-tetrakis(*p*-sulfonatophenyl) porphyrin doped hybrid borate glasses

N. Venkatramaiah^a, N. Veeraiah^b, R. Venkatesan^{a,*}

^a Department of Chemistry, School of Physical Chemical and Applied Sciences, Pondicherry University, R.V. Nagar, Puducherry 605014, India

^b Department of Physics, Acharya Nagarjuna University-Nuzvid Campus, Nuzvid 521201, A.P, India

ARTICLE INFO

Article history:

Received 14 August 2010

Received in revised form

11 November 2010

Accepted 15 November 2010

Available online 23 November 2010

Keywords:

Borate glass

Porphyrin

J-aggregates

Optical absorption

Luminescence

Dielectrics

ABSTRACT

Hybrid borate glasses containing different concentrations of *meso*-tetrakis(*p*-sulfonatophenyl) porphyrin sodium salt (TPPS₄) were prepared. The obtained glass samples were found to be transparent and homogeneous. Formation of TPPS₄-J-aggregates in borate glass was investigated by means of optical absorption, steady state and time resolved fluorescence spectroscopy. The hybrid glasses exhibit a strong S₂→S₀ emission at ~473 nm and J-aggregates show emission at ~733 nm. Time resolved fluorescence show two exponential decay with lifetime of $\tau_1 = 65 \pm 10$ ps (~80%) and $\tau_2 = 3.87 \pm 0.1$ ns (~20%) respectively. Dielectric properties such as dielectric constant (ϵ'), dielectric loss ($\tan \delta$) and ac conductivity (σ_{ac}) over a range of frequency and temperature of these glasses were studied. The ac conductivity was found to be proportional to ω^s (where $s < 1$). The observed change in dielectric parameters due to different concentrations of TPPS₄ has been analyzed in light of different polarization mechanisms.

© 2010 Elsevier B.V. All rights reserved.

1. Introduction

Low melting glasses with temperature less than 200 °C are desirable for many applications such as optical devices, moulding of optical elements, glass to metal seals and low temperature enamels for metals [1–3]. Recently, a new class of multifunctional materials, i.e., organic–inorganic hybrids is emerged, being a unique combination of organic chromophores into an inorganic oxide glass network [4,5]. The sol–gel process offers a method to incorporate organic dyes into inorganic matrices. The gels obtained are found to be porous and mostly resulted in dye leaching through pores and found to have limited heat treatment [6]. On the other hand, glasses obtained from melting methods are rigid and denser. Glasses like borate (B₂O₃), lead–tin–fluoro phosphate (PbF₂–SnF₂–SnO–P₂O₅) are the ideal low melting glasses and it is possible to integrate organic chromophores into these glasses without any decomposition [7–9]. Borate glasses are particularly interested due to presence of large number of trapping levels and show enhanced photo induced nonlinear optical effects [10,11]. It has been found that trapping of organic dyes in the rigid glassy network increase the longevity of the triplet state with significant population [12]. As a result of this, a large enhancement of third order nonlinear susceptibility $\chi^{(3)}$ in fluorescein, Rhodamine 6G doped borate glass films

as compared with solution medium and found potential applications in a variety of NLO devices [13–17].

Among many organic chromophores, porphyrins are attractive molecular dyes with flat and extended π -electron systems with rich electronic and redox properties [18–20]. *meso*-Tetrakis(*p*-sulfonatophenyl) porphyrin sodium salt (TPPS₄), a water soluble porphyrin of well defined molecular structure (Fig. 1) forms both H and J-aggregates depending on its electronic, stereo chemical, ionic strength and pH conditions [21–23]. The photophysical properties of TPPS₄ aggregates have been studied extensively *in vivo* or *in vitro* in important biological processes such as photodynamic therapy (PDT) [24,25]. Studies on interaction of self assembled nano structured aggregates with different π -electron systems can provide useful technological information. The structure, dynamic behaviour of the molecular aggregates and the conditions of aggregates formation, and their geometrical structures are of continuing interest [26].

Extensive research work on TPPS₄ and related macromolecules has been carried out in homogenous solutions, on flat crystalline mica, graphite, micelles and in polymers [27,28]. The photophysical properties of porphyrins in solid matrices especially in glassy matrix are limited due to the lack of suitable synthetic procedures. Investigation in this direction would help researchers to incorporate various organic molecules with predefined structures to tailor desired properties such as enhancement of conductivity. Further, it is quite likely that interaction between the borates and the organic molecules leads to the enhanced gradients of the ground state

* Corresponding author. Tel.: +91 413 2654415; fax: +91 413 2655987.

E-mail address: venkatesan63@yahoo.com (R. Venkatesan).

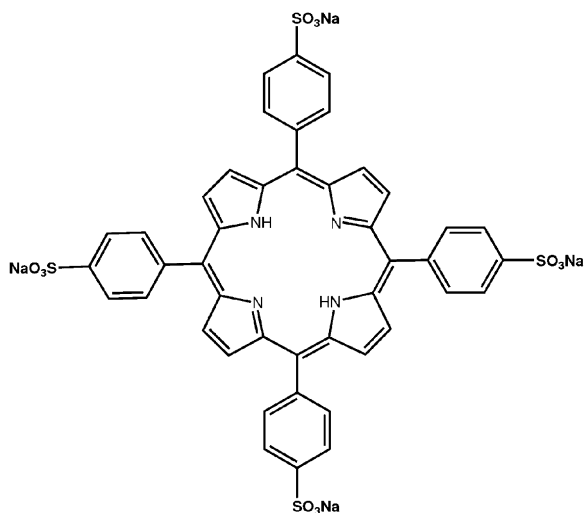


Fig. 1. The molecular structure of TPPS₄.

dipole moments leading to interesting changes in the dielectric and spectroscopic properties. The present study is therefore intended to prepare TPPS₄ doped hybrid borate glasses to investigate spectroscopic (viz., optical absorption, steady state emission, time resolved fluorescence) and dielectric properties to understand the structural influence on these properties and results are correlated with those in methanol medium.

2. Experimental methods

All the solvents and reagents were obtained from Himedia, India, and were used after purification. H₂TPPS₄Na₄ (TPPS₄) was prepared from the precursor *meso*-5,10,15,20-tetrakis(phenyl)porphyrin (H₂TPP) [29]. Weighed quantities of boric acid (12 g) and three different concentrations of TPPS₄ (ranging from 0.5 mg (P₁), 2 mg (P₂) and 3 mg (P₃)) were thoroughly mixed in an agate mortar and melted using a thick walled porcelain crucible at 150 °C in a proportional integral derivative (PID) temperature controlled furnace for about 5 h for decomposition of boric acid (H₃BO₃) to borate (B₂O₃). The temperature was rapidly raised to 230 °C to get the bubble free greenish melt. The resultant melt was poured on a preheated brass mould so as to obtain the circular glass discs of 2 mm thickness and 1 cm diameter. The obtained glasses were free from visible in-homogeneities, such as inclusions, cracks or bubbles. The glass discs thus obtained were annealed at 60 °C and subsequently polished with water-free lubricant such as diamond paste. The amorphous nature of the samples was studied by using Xpert PRO analytical X-ray diffractometer with Cu K α radiation. The surface morphology and homogeneous distribution of TPPS₄ in the glass sample was further confirmed by transmission electron microscopy (TEM; Technai F30). The density (ρ) of the glass samples was measured to an accuracy of ± 0.001 by the standard principle of Archimedes using *o*-xylene (99.99% pure) as the buoyant liquid. Differential scanning calorimetric analysis (DSC) of these samples was carried out by TA instruments Model Q20 V24.2 Build 107 with heating rate of 5 °C min⁻¹ in the temperature range 30–500 °C.

Optical absorption spectra of the hybrid glasses were recorded at room temperature with Ocean optics (HR4000) spectrophotometer. The FT-IR spectra were recorded in KBr method in the range 400–2000 cm⁻¹ using Nicolet 6700 FT-IR spectrometer. Steady state fluorescence emission was performed with a Spex FluoroLog-3 spectrofluorometer (Jobin-Yvon Inc.) equipped with a Hamamatsu R928 photomultiplier tube and double excitation and emission monochromators to a resolution of ± 1 nm. The phosphorescence emission was collected with IR sensitive photomultiplier by cooling with liquid nitrogen. Time resolved fluorescence measurements were performed using the time-correlated single-photon counting (TCSPC) with Nano LED (469 nm; FWHM < 200 ps) with repetition rate of 1 MHz was used to excite the samples. The photons collected at the detector were correlated by time to amplitude converter (TAC) to the excitation pulse. Signals were collected using an IBH Data station photon counting module and data analysis was performed using the commercially available DAS 6 software. The goodness of fit was assessed by minimizing the reduced χ^2 function and visual inspection of the weighted residuals with relative error of 5%. The dielectric measurements were made on LCR Meter (Hewlett-Packard Model-4263 B) in the frequency range 10² to 10⁵ Hz and in the temperature range 278–383 K. The accuracy in the measurement of dielectric constant is ~ 0.001 and that of loss is $\sim 10^{-4}$. A thin layer of silver paint was applied on either side of the large-faces of the samples, in order to serve as electrodes for dielectric measurements.

Table 1
Physical parameters of TPPS₄ doped borate glass.

Sample	Density (g/cm ³)	Molecular ion concentration (N _i) (mol/cm ³)	Inter molecular separation (R) (nm)	E _g (eV)	E _u (eV)
P ₁	1.866	2.94×10^{-17}	3.23	2.3	0.44
P ₂	1.886	11.78×10^{-17}	2.10	2.1	0.47
P ₃	1.916	17.68×10^{-17}	0.17	2.0	0.50

3. Results and discussion

From the measured values of density (ρ) and average molecular weight, various other physical parameters such as TPPS₄ molecular ion concentration (N_i) and intermolecular separation (R_i) are evaluated and presented in Table 1. The density of borate glass is found to be increased slightly with increase in the concentrations of TPPS₄ indicating an increase in the compactness of the glass material. Powder XRD pattern (Fig. 2) does not show any significant crystallinity in these materials. TEM picture (Fig. 3a) reveals aggregation of porphyrins and are arranged linearly on the glass surface. The EDS (Fig. 3b) spectra exhibit the characteristic elements such as B, O, C, N, S and Na distributed homogeneously in the glass sample. The FT-IR spectrum of TPPS₄ doped borate glass (Fig. 4) shows a characteristic signal at 1243 cm⁻¹, 807 cm⁻¹, 546 cm⁻¹ and another band at 445 cm⁻¹. These bands were identified as B–O bond stretching of the trigonal BO₃, vibrations of the BO₃ triangle, bending vibrations of the B–O–B linkages and B–O–B of boroxol ring deformations respectively [30]. No characteristic vibration pattern of TPPS₄ was observed due to its low concentration in the glass. The DSC profile (Fig. 5) of P₂ exhibits glass transition temperature (T_g) at 102 °C and an exothermic peak at 144 °C due to crystallization temperature (T_c) followed by endothermic peaks due to re-melting (T_m) at 172 °C. All hybrid glasses show similar behaviour for all concentrations of TPPS₄.

3.1. Optical absorption

The absorption spectrum of borate glass doped with different concentrations of TPPS₄ is presented in Fig. 6. The observed spectrum is completely different to that observed in methanol (inset of Fig. 6). The absorption spectrum of TPPS₄ in methanol solution exhibits four feeble characteristic bands at 500–650 nm region represented as Q band and one strong band near UV region at 415 nm called as Soret (B-band) band. However, all the TPPS₄ doped glass samples show three broad absorption peaks at ~ 432 nm, ~ 490 nm and ~ 705 nm. The observed red shift of the Soret band from 3.024 eV (in solution) to 2.863 eV (in the glass matrix) and appearance of new peaks at ~ 490 nm and ~ 705 nm indicate the formation of J-type aggregates of porphyrin [25]. This further reveals

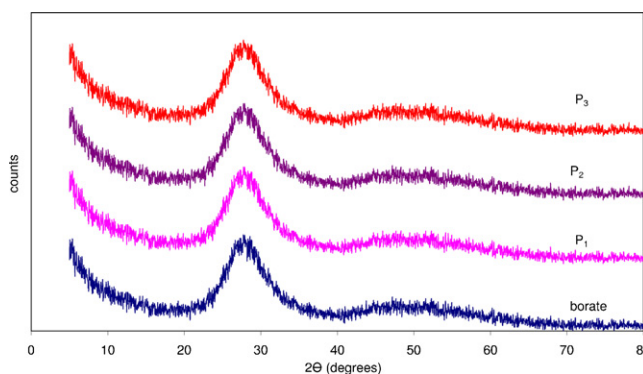


Fig. 2. Powder XRD pattern for different concentrations of TPPS₄ doped borate glass.

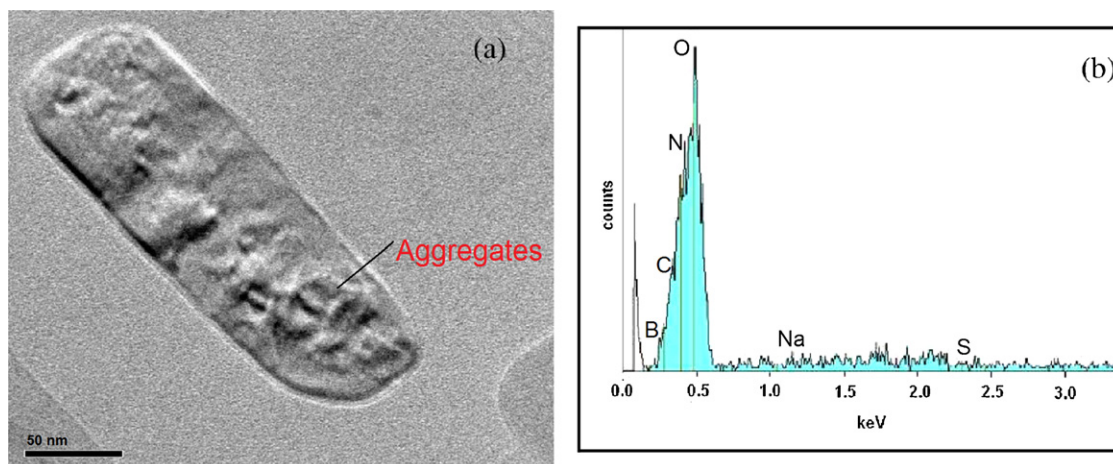


Fig. 3. (a) TEM and (b) EDS spectra of TPPS₄ doped glass (P₂).

that TPPS₄ reacts with borate glass during the melting process and undergone strong structural perturbation inside the glass matrix resulting in modification of the electronic absorption spectrum. Such perturbations can come from coordination of boron atoms with pyrrole nitrogens accompanied with distortion from porphyrin planarity [31]. The formation of J-aggregates occurs even at very low concentrations of TPPS₄ and the ratio between the intensities of absorption bands at ~490 nm and ~705 nm varies with concentration. The pertinent data of peak positions of various concentrations of TPPS₄ are summarized in Table 2. The FWHM of absorption band at 490 nm show more broader than its counterpart J-aggregates in solution [25]. Since, the glass quenching process evidently induces mechanical stresses and deformations of the aggregates causing the dispersion of excitonic interaction energies leading to broadening of absorption pattern as observed. Fig. 7 shows the optical band gap profile of TPPS₄ doped borate glasses. The dependence of the absorption coefficient (α) on the photon energy, $h\nu$, was represented by

$$(\alpha h\nu) = (h\nu - E_g)^n \quad (1)$$

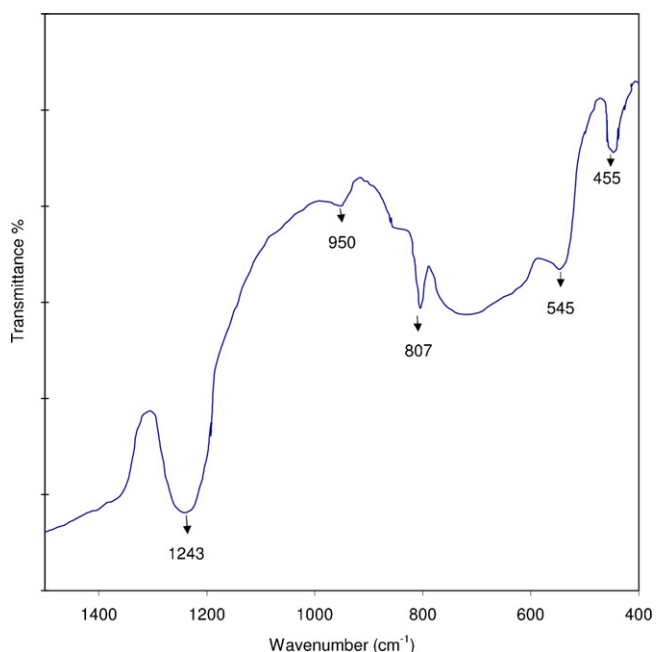


Fig. 4. FT-IR spectra of TPPS₄ doped borate glass (P₂).

From the extrapolation of the linear portion of the curves of Fig. 7, optical band gaps (E_g) were estimated and presented in Table 1. The E_g values are found to decrease with increase in the TPPS₄ concentration. The Urbach's energy (E_u) values were calculated as reciprocal gradient of straight line that is produced by a plot of natural logarithm of absorption coefficient $\ln(\alpha)$ on the photon energy as per the equation

$$\alpha = \alpha_0 \exp\left(\frac{E}{E_u}\right) \quad (2)$$

where α_0 is a constant and the E_u values show slight variation on increase of the concentration of TPPS₄. The change in the E_u values with composition is attributed to the potential fluctuations associated with chemical composition.

3.2. Steady state fluorescence emission

The steady state emission behaviour of TPPS₄ doped glasses is shown in Fig. 8, along with that observed in methanol. On excitation of TPPS₄ in methanol at $\lambda_{ex} = 415$ nm (inset of Fig. 8a), the emission spectrum shows two emission bands at 648 nm and 714 nm characteristic of $S_1 \rightarrow S_0$ transition and the emission is found to be independent of its excitation wavelength. In contrast to solution, on excitation at $\lambda_{ex} = 426$ nm, the glass samples show an intense emission at 473 nm along with two other peaks at 665 nm and 727 nm respectively (Fig. 8a). The fluorescence excitation spectra confirm that the former emission at 473 nm ($S_2 \rightarrow S_0$) and 665 nm ($S_1 \rightarrow S_0$) are associated with 426 nm absorption. On excitation at

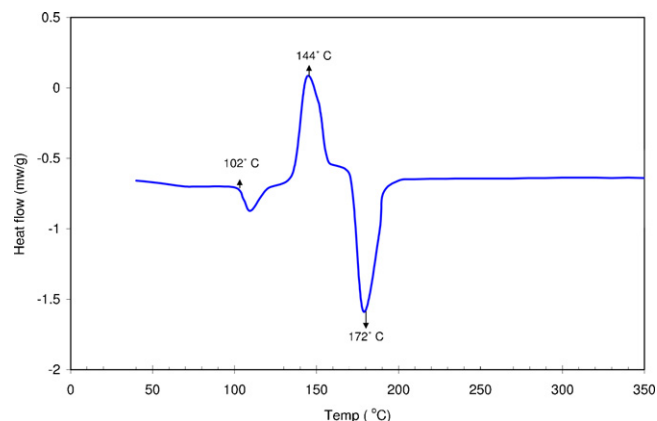


Fig. 5. DSC pattern of TPPS₄ doped glass (P₂).

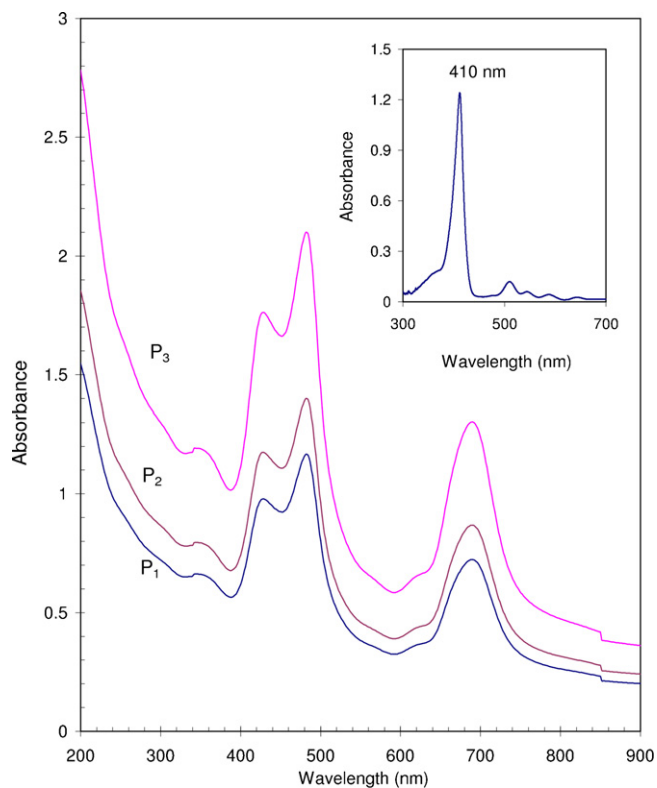


Fig. 6. Optical absorption spectra for different concentrations of TPPS₄ doped glasses. The inset in the figure shows the absorption spectrum of TPPS₄ in methanol.

$\lambda_{\text{ex}} = 490 \text{ nm}$ (Fig. 8b), the emission spectrum shows a distinct emission at $\sim 733 \text{ nm}$ is attributed to the fluorescence of J-aggregates [32]. The excitation and emission data for different concentrations of TPPS₄ in borate glasses are summarized in Table 2. The notable

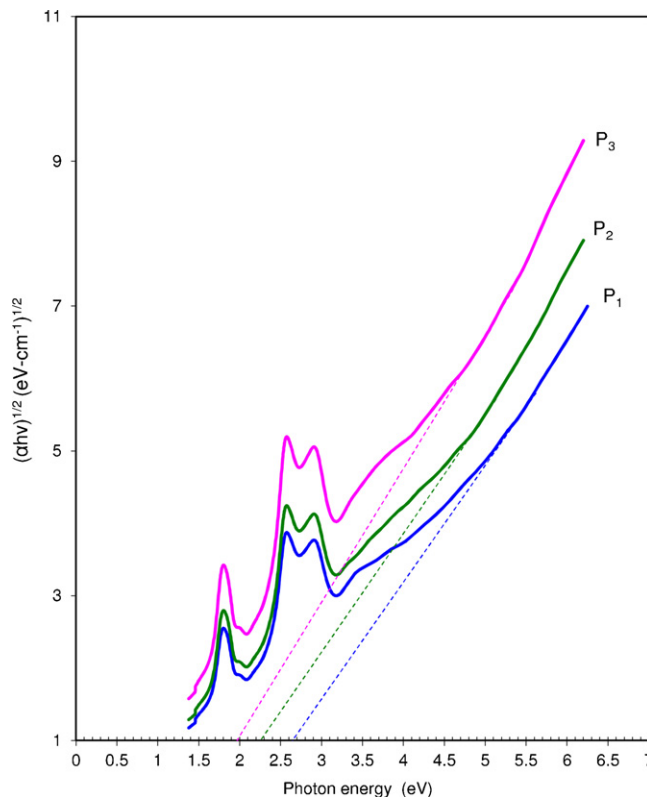


Fig. 7. The optical band gap profiles for different concentrations of TPPS₄ doped borate glasses.

feature from the emission spectra is the appearance of a strong $S_2 \rightarrow S_0$ emission and its intensity is found to be higher than that of $S_1 \rightarrow S_0$ emission. Normally, freebase porphyrins in the solution do not show $S_2 \rightarrow S_0$ emission (as is also observed in the present

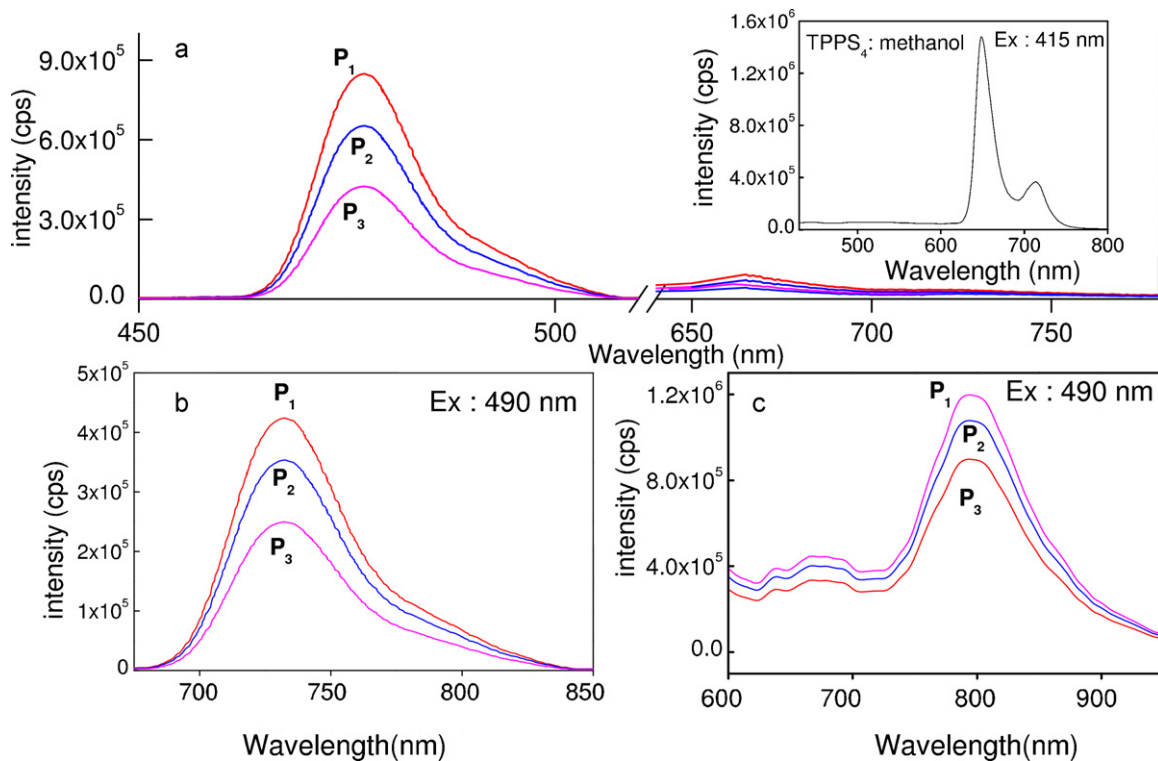


Fig. 8. (a) The fluorescence emission spectra of TPPS₄ in borate glass matrix at $\lambda_{\text{ex}} = 426 \text{ nm}$. The inset in the figure shows the emission spectra of TPPS₄ in methanol on excitation at $\lambda_{\text{ex}} = 415 \text{ nm}$. (b) The emission spectra of TPPS₄ in borate glass on excitation at $\lambda_{\text{ex}} = 490 \text{ nm}$. (c) The phosphorescence emission of TPPS₄ in borate glass on excitation at $\lambda_{\text{ex}} = 490 \text{ nm}$.

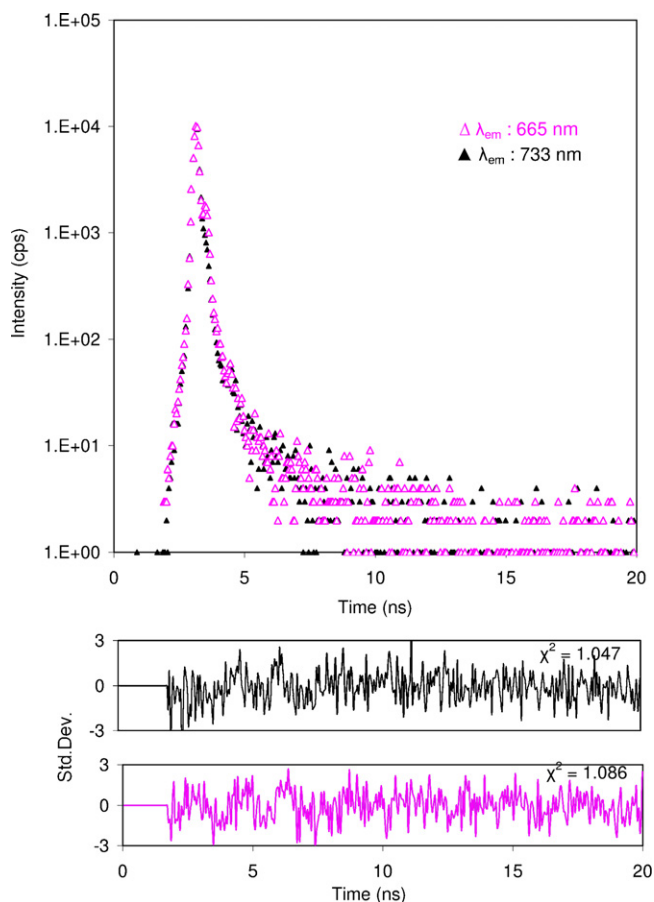


Fig. 9. Time resolved fluorescence decay of TPPS₄ in borate glass (P₂) for emission maxima (a) $\lambda_{em} = 665$ nm and (b) $\lambda_{em} = 733$ nm. The decay curves were fitted with bi-exponential function $I(t) = A + B_1 \exp(-t/\tau_1) + B_2 \exp(-t/\tau_2)$. The distribution of the weight residuals among the data channels corresponding to above fitting data and the χ^2 are given on the right top corner.

study (inset of Fig. 8a)) due to fast relaxation of electrons from S_2 to S_1 levels. However, $S_2 \rightarrow S_0$ emission was observed in Zn(II)TPP, Al(III)TPP(OH) in non polar solutions [33]. The appearance of $S_2 \rightarrow S_0$ emission in the glass further confirms the perturbation of porphyrin central core through boron bonding in the glass matrix. Also, increase in the amount of TPPS₄ in the glass matrix results decrease in the $S_2 \rightarrow S_0$ and $S_1 \rightarrow S_0$ emission intensities due to concentration quenching. The phosphorescence spectra (Fig. 8c) of J-aggregates exhibit broad emission at ~ 800 nm on excitation at 490 nm. The pertinent data of the phosphorescence emission and excitation data are summarized in Table 2. The large decrease in the $S_1 \rightarrow S_0$ emission and appearance of broad phosphorescence in the borate glass arises due to spin orbit coupling resulting from the interaction between triplet and singlet states of porphyrin.

3.3. Time resolved fluorescence emission

The fluorescence lifetime decay of TPPS₄ ($S_1 \rightarrow S_0$ emission) in borate glass is shown in Fig. 9 and the fitting data are summarized in Table 2. For all TPPS₄ doped glasses, the fluorescence decay profiles were found to fit for bi-exponential function that can be written as

$$I(t) = A + B_1 \exp\left(\frac{-t}{\tau_1}\right) + B_2 \exp\left(\frac{-t}{\tau_2}\right) \quad (3)$$

where $I(t)$ is the intensity at time t , A is constant, and B_1 , B_2 are the pre exponential factors (concentration terms) of lifetimes τ_1 and τ_2 respectively. All the glass samples showed distinct lifetimes $\sim \tau_1 = 65 \pm 10$ ps (80%) and $\sim \tau_2 = 3.87 \pm 0.1$ ns (20%) respectively.

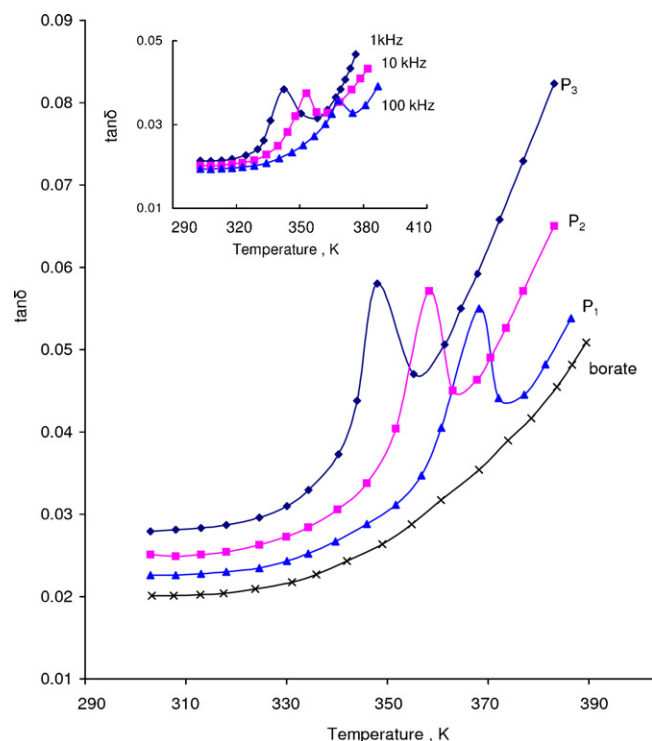


Fig. 10. A comparison plot of variation of dielectric loss with temperature for different concentrations of TPPS₄ doped glasses at 10 kHz. The inset in the figure shows the variation in the dielectric loss for P₂ at different frequencies.

The relative amplitudes of short and long lived species in the glass matrix remain constant with increase in the concentration of TPPS₄. This is in complete contrast to the observations of TPPS₄ in methanol where a single exponential decay with lifetime of ~ 10.112 ns. The presence of two distinct lifetimes indicates that two structurally different species exist in the glass matrix. The origin of the short lived species $\sim \tau_1 = 65 \pm 10$ ps is assigned as boron mediated J-aggregates of TPPS₄ and long lived species $\sim \tau_2 = 3.87 \pm 0.1$ ns to TPPS₄-borate complex [34]. The observed lifetime of J-aggregates in the glass is shorter than the J-aggregates of TPPS₄ (150 ps) in solution and in polymer matrix [35,36]. This suggests that the J-aggregates in the glass matrix undergo strong bimolecular exciton–exciton annihilation.

4. Dielectrics

Fig. 10 shows the variation of dielectric loss with temperature measured at 10 kHz for the samples doped with different concentrations of TPPS₄. The inset in figure shows the variation of $\tan \delta$ with temperature at different frequencies for sample P₂. The curves exhibit distinct maxima with shift of $(\tan \delta)_{max}$ towards higher temperature with increase in frequency. Such behaviour clearly indicates the dipolar relaxation character of dielectric loss. The activation energy evaluated from these curves shows a decrease in trend with increase in the concentration of TPPS₄ in the glass sample. This indicates that increase in the degree of freedom for dipoles to orient in the field direction due to the enhanced de-polymerization in the glass network. The pertinent values of $(\tan \delta)_{max}$ are summarized in Table 3. The temperature dependence of dielectric constant (ϵ') for TPPS₄ doped glasses is shown in Fig. 11. The inset in the figure shows dielectric constant for P₂ at different frequencies. From the figure, ϵ' decreases with the increase in frequency and increases with increase in temperature. Among various polarizations (electronic, ionic, dipolar and space charge polarization) that contribute to the dielectric constant, the

Table 2
The optical absorption, steady state and time resolved fluorescence and phosphorescence emission data of TPPS₄ doped in borate glass.

Sample	Absorption (nm)	Fluorescence emission		Phosphorescence emission			Fluorescence lifetime		χ^2
		λ_{ex} (nm)	λ_{em} (nm)	λ_{ex} (nm)	λ_{em} (nm)	$\Delta\lambda$ (nm)	τ_1 (ns)	τ_2 (ns)	
P ₁	429,491,696	426	473,665,724	–	–	–	0.063 (76.38)	3.861 (23.62)	1.029
		490	733	490	791	22.65	0.085 (86.23)	3.942 (13.77)	1.112
P ₂	430,493,704	426	475,665,727	–	–	–	0.068 (82.16)	3.934 (17.84)	1.086
		490	733	490	794	22.95	0.089 (88.19)	3.986 (11.81)	1.047
P ₃	433,495,709	426	476,665,727	–	–	–	0.072 (84.54)	3.921 (15.46)	1.044
		490	735	490	795	23.8	0.091 (89.67)	3.991 (10.33)	1.141
Methanol	410,515,550,593,648	415	648,714	–	–	–	–	10.112 (100)	1.015

Table 3
Results on dielectric loss of TPPS₄ doped in borate glasses.

Sample	Activation energy for dipoles (eV)	$(\tan \delta_{max})_{avg}$	Temp. region of relaxation (K)
P ₁	0.623	0.055	360–372
P ₂	0.611	0.057	351–368
P ₃	0.602	0.058	344–358

space charge polarization will depend on the nature of modifying ions in the glass network. The observed ϵ' is due to contribution of multi-components of polarizability, deformational polarization and relaxation polarization (orientational and interfacial). From the figure, ϵ' increases with the increase in temperature and exhibits strong temperature dependence at higher temperature and lower frequencies. The increase of ϵ' with temperature can be attributed to the space charge connected with depolymerization of borate glass network.

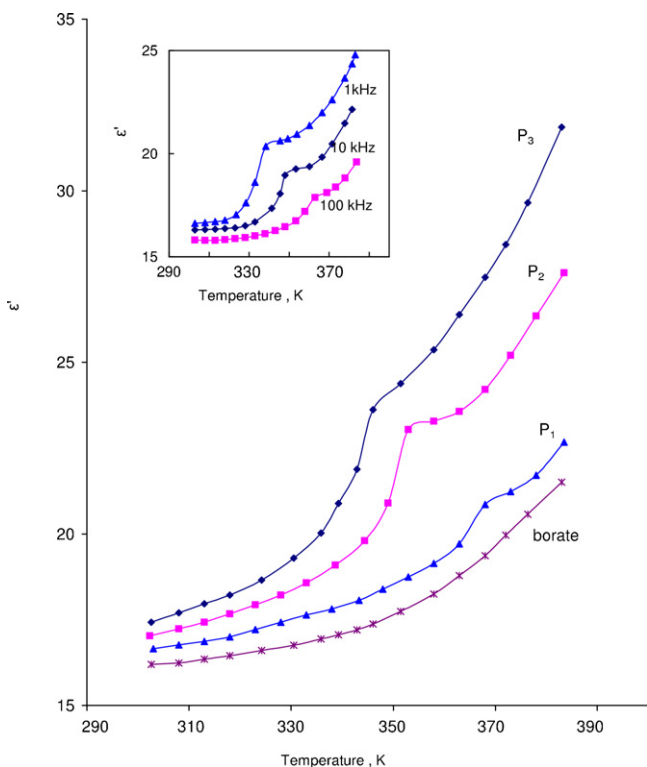


Fig. 11. A comparison plot of variation of dielectric constant with temperature for different concentrations of TPPS₄ doped glasses at 10 kHz. The inset in the figure shows the dielectric constant of P₂ at different frequencies.

The ac conductivity $\sigma_{ac}(\omega)$ was calculated at different temperatures using the expression

$$\sigma_{ac} = \omega \epsilon' \epsilon_0 \tan \delta \quad (4)$$

where ϵ_0 is the vacuum dielectric constant. Fig. 12 shows the variation of ac conductivity with $1/T$ for the glasses doped with different concentrations of TPPS₄ at 10 kHz. The plot of $\log \sigma_{ac}$ against $1/T$ for all TPPS₄ doped glasses show increase in the conductivity as amount of TPPS₄ increased. The inset in Fig. 12 shows the variation of $\log \sigma_{ac}$ with $1/T$ for sample P₂ at different frequencies. The activation energy (A.E.) for the conduction in the high temperature region over which linear dependence of $\log \sigma_{ac}$ with $1/T$ is evaluated and presented in Table 3. Such behaviour indicates that ac conductivity is a thermally activated process from different localized states in the gap. The activation energy is found to decrease with increase in the content of TPPS₄. Further, the variation of σ_{ac} with activation energy shows linear dependency (inset b of Fig. 10). The universal character of the frequency dependent conductivity is preserved for

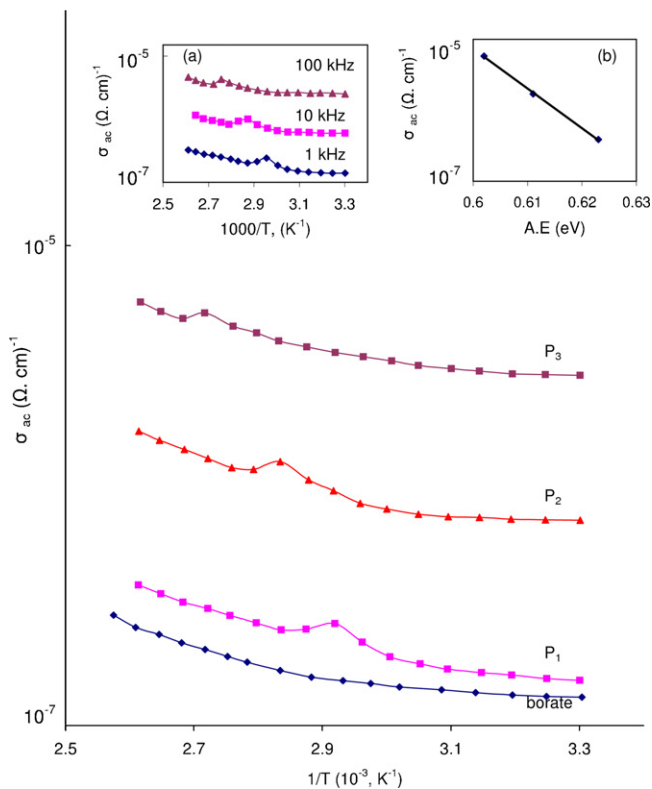


Fig. 12. A comparison plot of variation of ac conductivity with $1/T$ at 10 kHz for different concentrations of TPPS₄ doped glasses. Inset (a) gives the ac conductivity of P₂ at different frequencies and (b) gives the variation of conductivity with the activation energy.

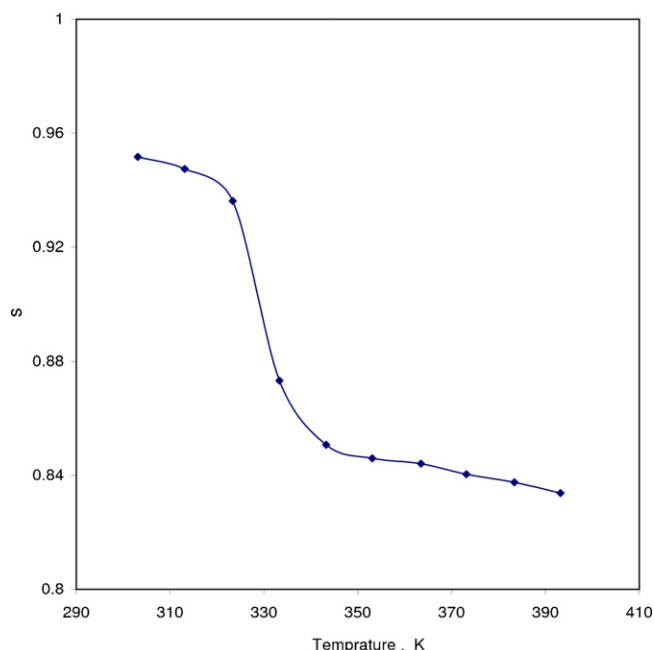


Fig. 13. The temperature dependence of the parameter s for TPPS₄ doped glass P₂.

the wide range of amorphous materials. The ac conductivity $\sigma_{ac}(\omega)$ increases with frequency according to the equation

$$\sigma_{ac}(\omega) = A\omega^s \quad (5)$$

where ω is the angular frequency, $\omega = 2\pi f$, A is constant which is independent of temperature and s is frequency exponent. The values of s were calculated from the slopes of the straight lines for all investigated samples at different temperatures by using logarithmic form of Eq. (5). At low frequencies, the exponent s is less than unity and decreases with increase in temperature as shown in Fig. 13. According to correlated barrier hopping (CBH) model, the values of frequency exponent s decrease from 1.0 to 0.7 with increase in temperature. This indicates that correlated barrier hopping mechanism is dominant in these hybrid materials [37]. The theoretical expression for s derived on the basis of CBH model by Elliot is

$$s = 1 - \frac{6KT}{E_g} \quad (6)$$

where K is Boltzman constant, T is the temperature in Kelvin and E_g is the optical band gap of the material. From Eq. (6), the average value of s at room temperature ($T = 303$ K) is ≈ 0.65 . The difference between the calculated and measured values of s is due to hopping of organic compounds likely to be greater complexity than in oxide films [38,39].

5. Conclusions

TPPS₄ doped hybrid borate glasses were successfully prepared for the first time by melt quench technique. The XRD pattern reveals the amorphous nature of the hybrid glasses. The TEM and EDS analysis confirmed the retention of all elements and homogeneous distribution in the glass sample and the aggregates are arranged in discrete manner. The optical absorption spectrum shows appearance of new peaks at ~ 430 nm, ~ 490 nm and ~ 700 nm indicating the formation of TPPS₄-J-aggregates in the borate glass. The appearance of strong $S_2 \rightarrow S_0$ fluorescence emission at ~ 473 nm and decrease in the $S_1 \rightarrow S_0$ fluorescence emission intensity reveals that

structure of TPPS₄ was inherently modified through boron atoms of borate network and strong perturbation occurs at the central core. The decrease in fluorescence lifetime decay of TPPS₄ J-aggregates shows that decrease in the vibrational deactivation pathway by N-B vibrations due to inherent modifications during the glass formation. The ac conductivity (σ_{ac}) was found to be varying as ω^s in the frequency range 10^2 to 10^5 Hz. The frequency exponent s is less than unity and decreases with increase in the temperature indicating correlated barrier hopping (CBH) is dominant in the hybrid glasses.

Acknowledgements

RV is thankful to the Council of Scientific and Industrial Research (CSIR), Govt. of India, New Delhi, for funding the research project (01(2087)/06/EMR-II). NVR thank CSIR, New Delhi for providing SRF fellowship. The authors are also grateful to Central Instrumentation Facility (CIF), Pondicherry University for providing the instrumentation facility. RV also acknowledge to Prof. P. Ramamurthy and Dr. C. Selvaraju, National Centre for Ultrafast Processes (NCUFP), Chennai for recording pico-second lifetime.

References

- [1] L.M. Sanford, P.A. Tick, US Patent no. 4,314,021 (1982).
- [2] P. Colomban, J. Nano Res. 8 (2009) 109.
- [3] R. Suzuki, S. Takei, E. Tashiro, K. Machida, J. Alloys Compd. 408–412 (2006) 800.
- [4] M. Pędziwiatr, R. Wiglusz, A. Graczyk, J. Legendziewicz, J. Alloys Compd. 451 (2008) 46.
- [5] L. Weia, Q. Chena, Y. Gu, J. Alloys Compd. 501 (2010) 313.
- [6] R. Makote, M.M. Collinson, Anal. Chim. Acta 394 (1999) 195.
- [7] L.R. Avila, E.C. de, O. Nassor, P.F.S. Pereira, A. Cestari, K.J. Ciuffi, P.S. Calefi, E.J. Nassar, J. Non-Cryst. Solids 354 (2008) 4806.
- [8] S. Jiang, T. Luo, J. Wang, J. Non-Cryst. Solids 263–264 (2000) 358.
- [9] J.M. Oreilly, K. Papadopoulos, J. Mater. Sci. 36 (2001) 1595.
- [10] I.V. Kityk, A. Majchrowski, W. Imiolek, E. Michalski, Opt. Commun. 219 (2003) 421.
- [11] A. Majchrowski, J. Ebothe, E. Gondek, K. Ozga, I.V. Kityk, A.H. Reshak, T. Lukasiewicz, J. Alloys Compd. 485 (2009) 29.
- [12] W.R. Tompkin, R.W. Boyd, D.W. Hall, P.A. Tick, J. Opt. Soc. Am. B 4 (1987) 1030.
- [13] R.C. Sharma, Spectrochim. Acta A 69 (2008) 800.
- [14] R.C. Sharma, T.A. Waigh, J.P. Singh, Opt. Commun. 281 (2008) 2985.
- [15] J. Humphrey, D. Kuciauskas, J. Phys. Chem. B 108 (2004) 12016.
- [16] K. Divakar Rao, S. Anantha Ramakrishna, P.K. Gupta, Appl. Phys. B 72 (2001) 215.
- [17] K. Kandasamy, K. Divakar Rao, R. Deshpande, P.N. Puntambekar, B.P. Singh, S.J. Shetty, T.S. Srivastava, Appl. Phys. B 64 (1997) 479.
- [18] M. Gouterman, in: D. Dolphin (Ed.), The Porphyrins Physical Chemistry Part A, Academic Press, New York, 1978.
- [19] K. Smith, Porphyrins and Metalloporphyrins, Elsevier/North Holland Biomedical Press, Amsterdam, 1976.
- [20] P. Prasad, D. William, Introduction to Nonlinear Optical Effects in Molecules and Polymers, Wiley, New York, 1991.
- [21] L. Guo, J. Colloid Interface Sci. 332 (2008) 281.
- [22] L.P.F. Aggarwal, I.E. Borissevitch, Spectrochim. Acta B 63 (2006) 227.
- [23] R.F. Pasternack, K.F. Schaefer, H. Hambright, Inorg. Chem. 33 (2002) 2065.
- [24] M. Ochsner, J. Photochem. Photobiol. 62 (1997) 1.
- [25] N.C. Maiti, M. Ravikanth, S. Mazumdar, N. Periasamy, J. Phys. Chem. 99 (1995) 17192.
- [26] G. De Luca, A. Romeo, L.M. Scolaro, J. Phys. Chem. B 110 (2006) 7309.
- [27] R. Rotomskis, R. Augulis, V. Snitka, J. Phys. Chem. B 108 (2004) 2833.
- [28] V. Snitka, M. Rackaitis, R. Rodaite, Sens. Actuators B: Chem. 109 (2005) 159.
- [29] G. Meng, B.R. James, K.A. Skov, M. Korbelik, Can. J. Chem. 72 (1994) 2447.
- [30] W.A. Pisarski, J. Pisarska, W.R. Romanowski, J. Mol. Struct. 744–747 (2005) 515.
- [31] D. Mohajer, S. Zakav, S. Rayati, M. Zahedi, N. Safari, H. Reza khavasi, S. Shahbazian, New J. Chem. 28 (2004) 1600.
- [32] J. Valanciunaite, S. Bagdonas, G. Streckyte, R. Rotomskis, Photochem. Photobiol. Sci. 5 (2006) 381.
- [33] Y. Kurabayashi, K. Kikuchi, H. Kokubun, Y. Kaizu, H. Kobayashi, J. Phys. Chem. 88 (1984) 1308.
- [34] N. Venkatramaiah, R. Venkatesan, Mater. Chem. Phys. 125 (2011) 729.
- [35] V. Gulbinasa, R. Karpicz, R. Augulis, R. Rotomskis, Chem. Phys. 332 (2007) 255.
- [36] L. Kelbauskas, S. Bagdonas, W. Dietel, R. Rotomskis, J. Lumin. 101 (2003) 253.
- [37] S.R. Elliot, Philos. Mag. 36 (1977) 1291.
- [38] N.S. Yesugade, C.D. Lohane, C.H. Bhosale, Thin Solid Films 263 (1995) 145.
- [39] R.D. Gould, A.K. Hassan, Thin Solid Films 223 (1993) 334.